GSA Data Repository 2016337

"Pseudotachylyte Increases the Post-Slip Strength of Faults"

B. Proctor* and D. Lockner

*To whom correspondence should be addressed. Email: bproctor@usgs.gov

This file includes text, figures and one table that are divided into eight repository items:

Data Repository Item DR1

Deformation Apparatus, data reduction and methods

Experiments were performed in a conventional triaxial apparatus (similar to the machine used in *Lockner et al.*, 2016). Axial stress was measured with an external load cell and corrected for seal friction, which ranged from 2.5 to 4.5 % of the confining pressure. Axial displacement (z) was measured with and external DCDT sensor. Shear stress (τ), normal stress (σ_n), fault slip (δ) and friction (μ) values were calculated following methods reported in *Lockner et al.*, 2016. A shear stress correction was made for the elasticity of the polyurethane jacket, which was determined to be ~0.35 MPa/mm axial displacement. Fault slip was not measured directly.

Reported values are computed from the external axial displacement record by correcting for elastic shortening of the sample column: $\delta = (z - \tau/k)/\cos\theta$, where k is the nominal stiffness (126 MPa/mm) and $\cos\theta$ accounts for the inclined fault surface. For the energy density calculations, fault area (A) was assumed to be 0.001 m^2 (see text). Confining pressure precision is ±0.1 MPa and accuracy is ±0.3 MPa. Axial and differential stresses have precision of ±0.1 MPa and accuracy of ±0.2 MPa or ±0.2 %, whichever is greater. Displacement precision is ±0.2μm and accuracy is 0.5% (*Lockner et al*., 2016).

During the strength recovery tests (see text) a constant normal stress was imposed. To achieve a constant normal stress, we used a computer controlled system that conducts a real time calculation of normal stress during deformation [see *Tembe et al.*, 2010]. In response to changing axial stress the system automatically adjusted the confining pressure to either raise or lower the normal stress. The response time is on the order of one second.

To improve the axial alignment prior to deformation the prepped samples were first jacketed with a 0.025 mm-thick copper sleeve. They were next placed in a polyurethane jacket, compressed under 100 MPa of hydrostatic pressure in a kerosene-filled pressure vessel and quickly removed from pressure. We next ground the ends of the Cu-jacketed sample parallel using a surface grinder. Finally, the samples were placed in a vacuum oven at ~80 C for at least 2 hours to remove any water that may have accumulated inside the copper jacket. The Cu-jacket has a negligible contribution to the measured sample strength at the conditions explored in this study.

Data Repository Item DR2

Summary of experimental conditions

All experimental conditions are listed in Table DR1.

Table DR1. Experimental Conditions

Run #	Confining Pressure (MPa)	Axial Loading Rate (μm/s), Pore Pressure (MPa)	Strength Recovery Test Normal Stress/Confining Pressure (MPa)	Strength Recovery Test Loading Rate (μm/s), Pore Pressure (MPa)
12	400	5, 0	-	-
13	200	5, 0	-	-
14	200	5, 0	-	-
15	100	5, 0	-	-
16	420	5, 20	-	-
17	210	5, 10	-	-
18	105	5, 5	-	-
19	50	5, 0	-	-
20	105	5, 0	-	-
21	100	5, 0	-	-
23	52.5	5, 2.5	-	-
27	400	5, 0	-	-
29	200	5, 0	-	-
30	210	5, 10	-	-
31	200	5, 0	50	5, 0
32	210	5, 10	50	5, drained
34	400	5, 0	50	5, 0
35	420	5, 20	50	5, drained
36	400	5, 0	60	1, 0
37	420	5, 20	80	1, 20
38	300	5, 0	60	1, 0
39	315	5, 15	60	1, 3
41	420	5, 20	63	1, 3
42	400	5, 0	60	1, 0
43	60-31*	1, 0	60	-
45	400	5, 0	60	1, 0
46	400	5, 0	60	1, 0
47	300	5, 0	60	1, 0
48	200	5, 0	60	1, 0
49	200	5, 0	60	1, 0
50	100	5, 0	60	1, 0
51	100	5, 0	60	1, 0
52	210	5, 10	63	1, 3
53	105	5, 5	63	1, 3
54	50	5, 0	60	1, 0
55	52.5	5, 2.5	63	1, 3
56	200	5, 0	60	1, 0

Data Repository Item DR3

Description of starting material

Westerly granite was collected from a quarry in Westerly, Rhode Island and has been described in numerous studies [e.g., *Tullis and Yund*, 1977]. A photograph of a sawcut surface is shown in Figure DR1 along with photomicrographs of the slip surface.

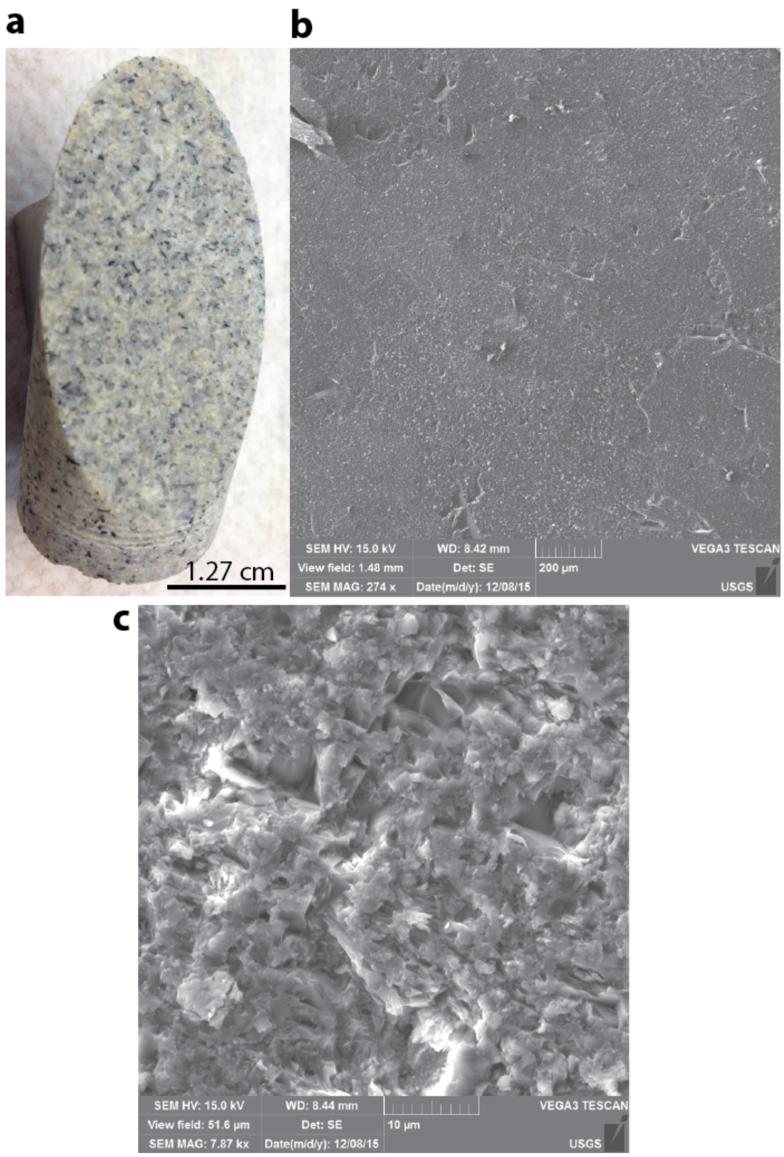

Figure DR1. Images of the starting surface. (a) Photomicrograph of the slip surface prior to deformation. (b) SE-SEM image of the slip surface with a 600 grit polish (see Methods section). The surface is mostly flat with a uniform polish; in a few places grains or pieces of grains were plucked from the surface leaving small holes. (c) SE-SEM image of the slip surface showing a roughness on the order 1-5 µm.

Data Repository Item DR4

Catalog of mechanical data

In Figure DR2 we present reduced shear stress data versus on fault slip for all experiments.

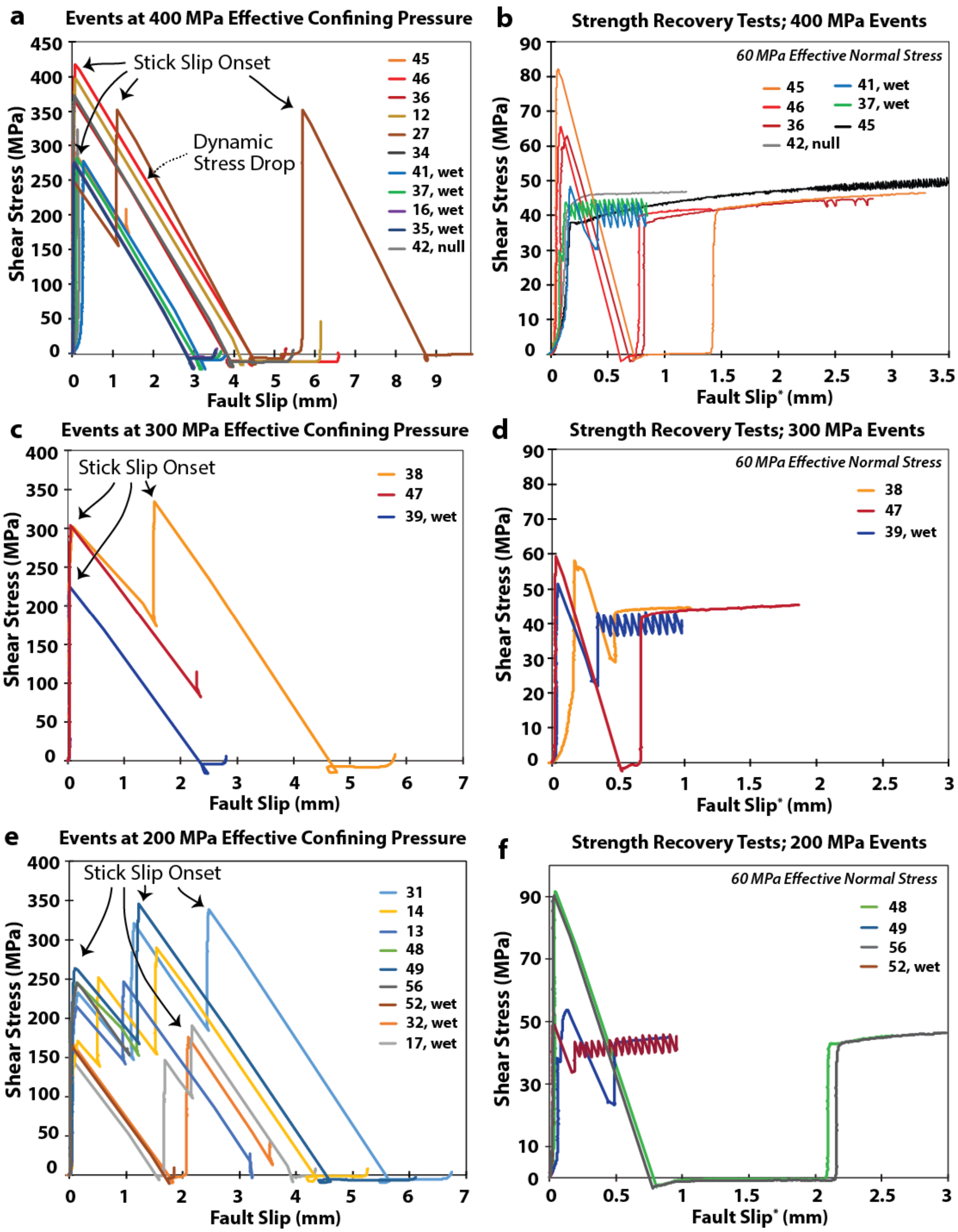

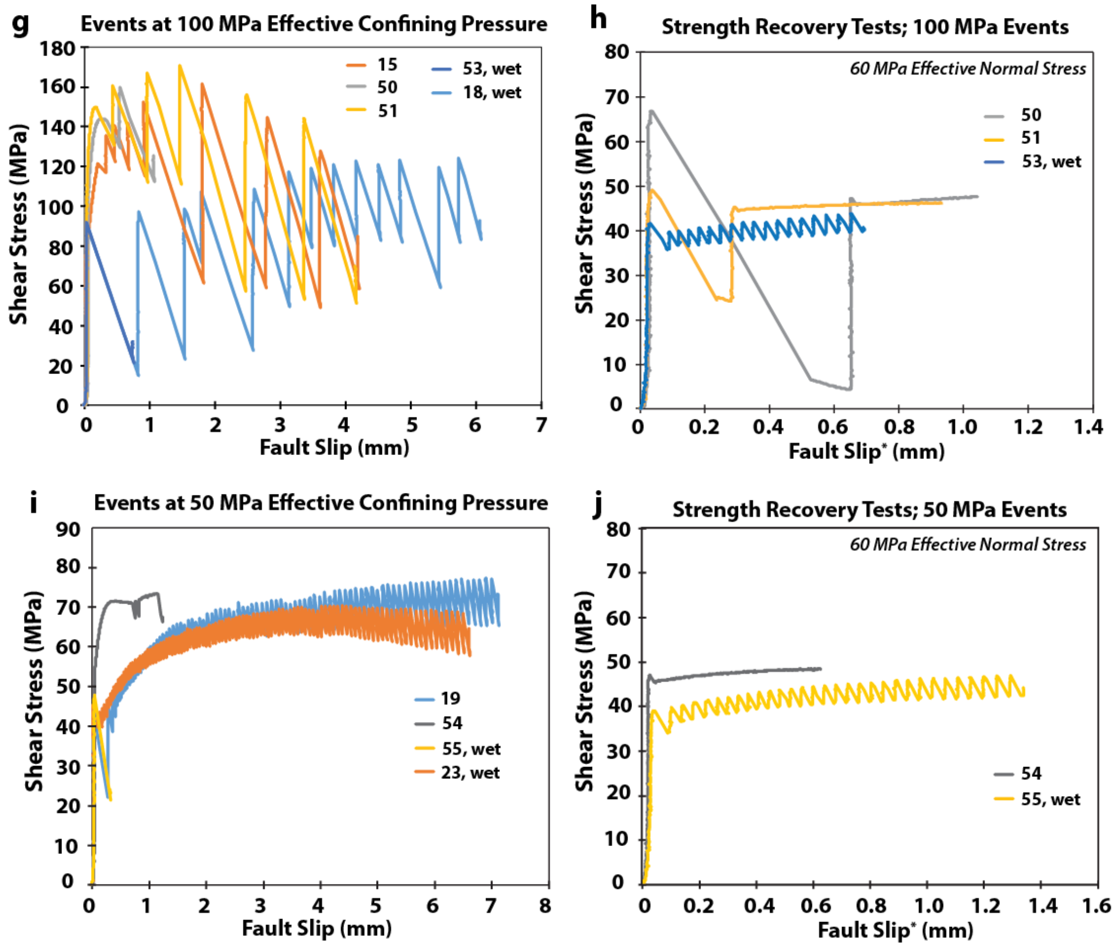

Figure DR2 (a-j). Graphs of resolved shear stress and displacement data from experiments reported in this study. Panels are separated by the applied confining pressure (left) or normal stress (right, noted in italic). The strength recovery test data (right) are separated into panels following the corresponding slip event data (left). *The fault slip values for strength recovery tests were set to zero, however the actual slip value at the onset of the strength test can be observed in the corresponding event panels.

Data Repository Item DR5

Additional observations of of experimental microstructures

In Figure DR3 we present additional microstructural images from deformed samples.

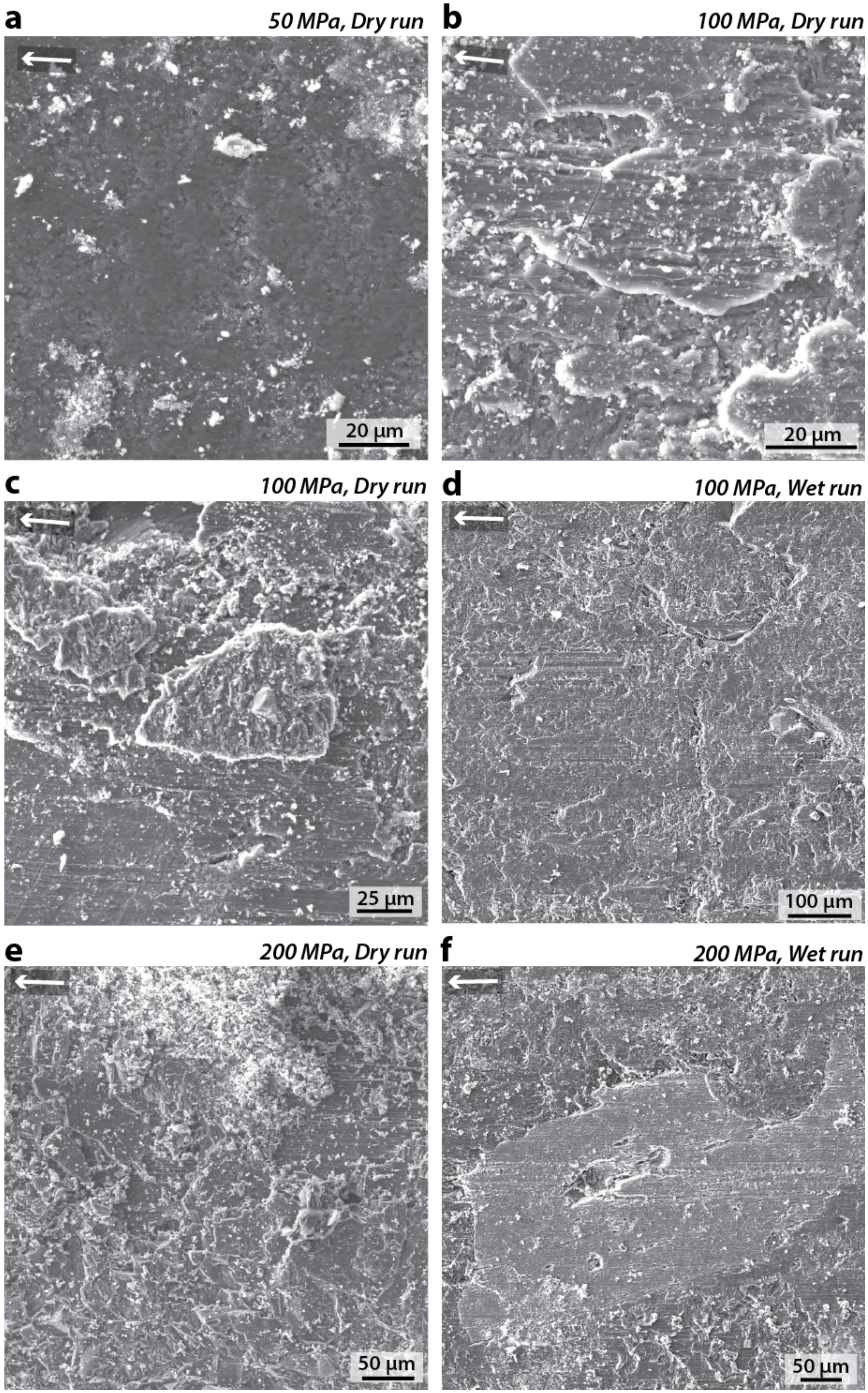
a
50 MPa, Dry run
20 µm
b
100 MPa, Dry run
20 µm
c
100 MPa, Dry run
25 µm
d
100 MPa, Wet run
100 µm
e
200 MPa, Dry run
50 µm
f
200 MPa, Wet run
50 µm

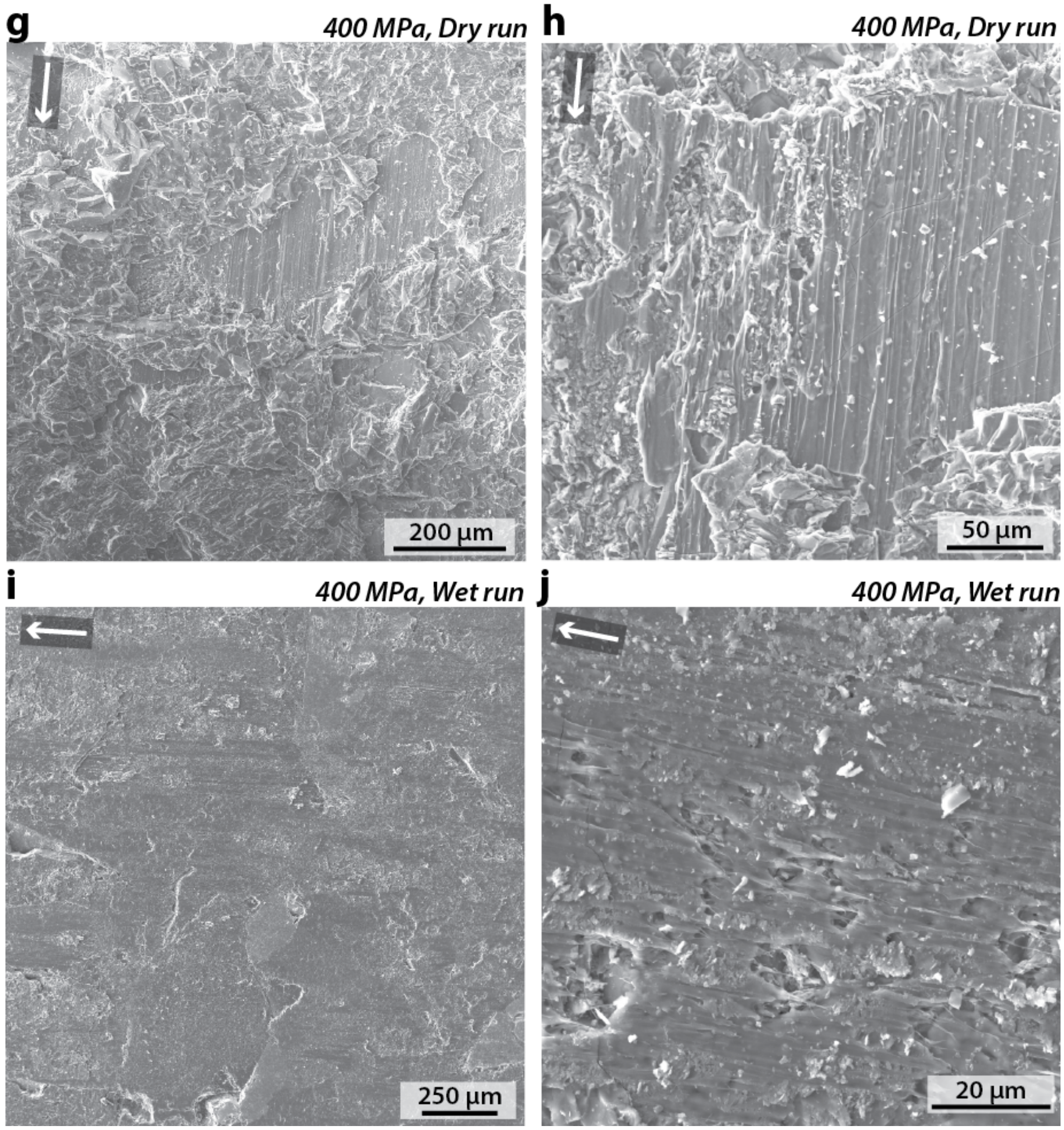

Figure DR3 (a-j). SE-SEM images of the slip-surface deformed at different experimental conditions. White arrows indicate the approximate slip direction of the observed shearing surface. The applied confining pressure and and wet/dry conditions are noted in italic. (a) Partially polished section of the slip surface (compare with Supplemental Fig. 4b) with no evidence of melt material; Run 19. (b) Patches of melt material on the slip surface, some overprinting one another; Run 15. (c) Image shows regions of the slip surface covered with melt material with striations. The center and upper left show partial sections of the opposing slip surface welded to the facing surface; Run 15. (d) Striated and mostly flat slip surface void of welded structures (compare with panel c); Run 18. (e) Section of slip surface that is mostly covered with welded sections of the opposing slip surface; Run 14. (f) Striated and mostly flat region void of welded structures (compare with panel e); Run 17. (g) Region that is mostly covered with welded sections of the opposing slip surface; Run 12. (h) Enlarged region of the surface where melt material is observed; Run 12. (i) Striated and mostly flat region void of welded structures (compare with panel g); Run 16. (j) Enlargement of surface showing melt material with entrained gouge and flow structures with top to the right sense of shear; Run 16.

Data Repository Item DR6

Correlation between peak stress, slip and gouge

In Figure DR4 we show the correlation between peak stress values measured during the strength recovery tests and the amount of slip prior to the tests. Figure DR5 shows how the amount of apparent surface gouge increases with slip (see text).

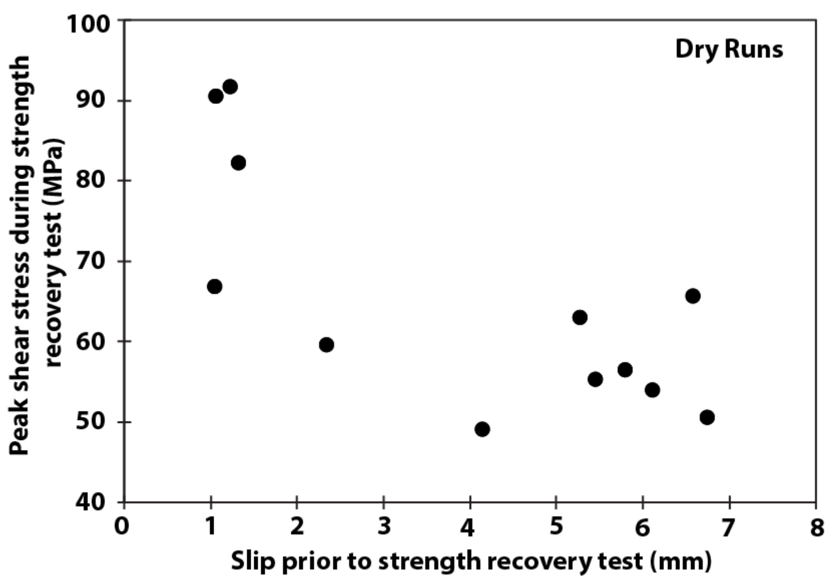

Figure DR4. Plot of peak shear stress values measured during strength recovery tests of dry samples versus the total slip that occurred prior to the SR test. The plot shows that runs with more displacement have increasingly lower peak stress values.

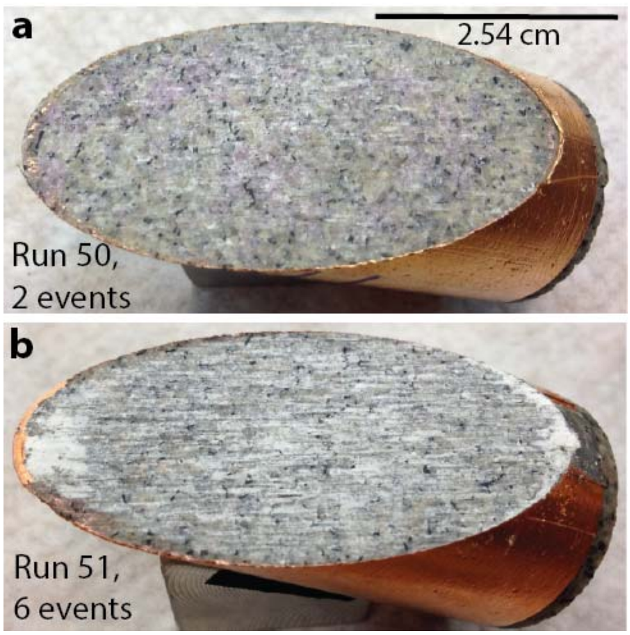

Figure DR5. Photomicrographs of samples deformed at 100 MPa confining pressure. (a) Image shows very little accrued gouge (white powder) after deformation. (b) Image shows a noticeable amount of gouge on surface occurring primarily along striations paralleling the slip direction. The concentrated zones of gouge near the toe and heel of the sample likely accumulated when the sample was removed from the polyurethane jacket.

Data Repository Item DR7

Plots of fault creep prior to stick-slip sliding

Our results show significant differences in the amount of fault creep prior to the onset of stick-slip events between wet and dry samples. Fault creep represents stable frictional sliding in which we typically observe an increase in shear stress with slip. Figure DR6 plots the shear stress record over the first few tenths of a millimeter of slip. This plot demonstrates that dry samples almost always exhibit more fault creep than wet sample at all confining pressures tested.

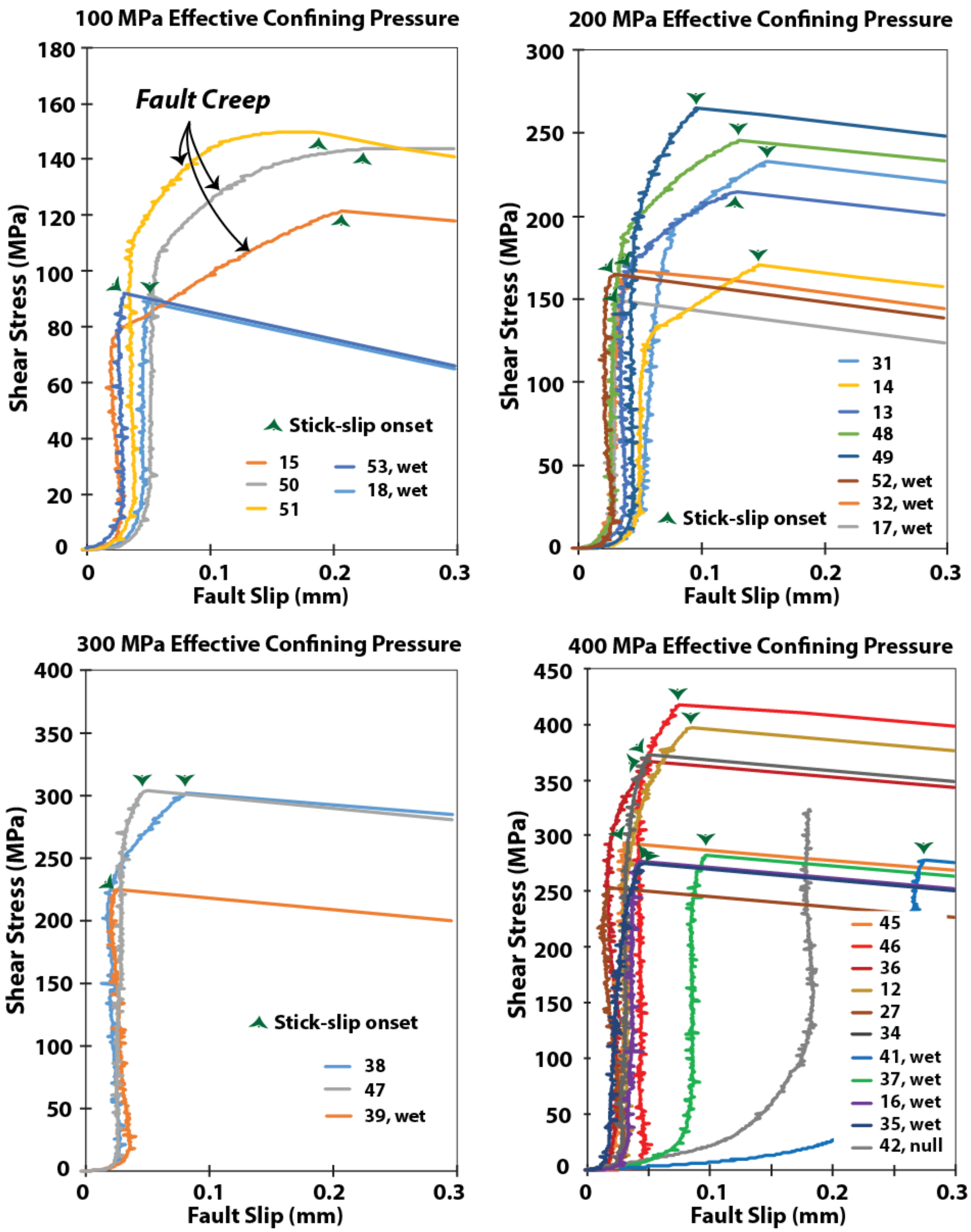

Figure DR6. Loading profiles prior to the first stick-slip events. Samples are grouped by the imposed confining pressure, from 100-400 MPa. Dry samples typically undergo inelastic fault creep concomitant with work hardening before a stick-slip event is nucleated. Conversely, wet samples undergo very little fault creep or work hardening prior to the onset of stick-slip events.

References Cited in Data Repository

Lockner, D. A., B. D. Kilgore, N. M. Beeler and D. E. Moore, 2016, The transition from frictional sliding to shear melting in laboratory stick-slip experiments, AGU monograph series, Fault zone properties, (Accepted May 2016)

Tembe, S., Lockner, D. A. and Wong T.-F, 2010, Effects of clay content and mineralogy on frictional sliding behavior of simulated gouges: Binary and ternary mixtures of quartz, illite, and montmorillonite, *J. Geophys. Res.*, 115, B03416.

Tullis, J.and R. A. Yund, 1977, Experimental deformation of dry Westerly granite, *J. Geophys. Res, 82*(36), 5705-5718.